

Article

Feedback control for biomechanical systems in the presence of asynchronous sampling based on high-gain observers

Liangping Cheng*, Niannian Yan

Chongqing University of Education, Chongqing 400000, China

* **Corresponding author:** Liangping Cheng, cheng_liangping@163.com

CITATION

Cheng L, Yan N. Feedback control for biomechanical systems in the presence of asynchronous sampling based on high-gain observers. *Molecular & Cellular Biomechanics*. 2025; 22(4): 1450. <https://doi.org/10.62617/mcb1450>

ARTICLE INFO

Received: 3 March 2025
Accepted: 7 March 2025
Available online: 24 March 2025

COPYRIGHT



Copyright © 2025 by author(s).
Molecular & Cellular Biomechanics is published by Sin-Chn Scientific Press Pte. Ltd. This work is licensed under the Creative Commons Attribution (CC BY) license. <https://creativecommons.org/licenses/by/4.0/>

Abstract: In this paper, the problem of designing an asynchronous sampling observer and controller for the biomechanical nonlinear systems is investigated. The central nervous system controls biomechanical limb movements through complex neurophysiological mechanisms. The state sampling input observation obtained by the proprioceptor exhibits asynchronous phenomena when transmitted to the central nervous system. The observation information about parts of the body suffers unmodeled dynamics and nonlinear dynamics in transmissions to the central nervous system. Firstly, unmodeled dynamics are introduced to a class of biomechanical hybrid systems, which can be mitigated by increasing the gain of the observer. The high-gain observer designed can solve the problem of obtaining the state information of various parts of the human body and analyze the stability of the error system. Then, the asynchronous sampling controller is structured to realize the nervous system feedback control based on the high-gain observer. Sufficient conditions for the existence of controllers for observer-based sampled data in discrete time are obtained by using the Lyapunov functions and separation principle. Finally, the effectiveness of the method is illustrated by a numerical example.

Keywords: biomechanical limbs movement; central nervous system; unmodeled dynamics; high-gain observer; feedback control

1. Introduction

The theory of optimal control plays a key role in the study of biological motion. In recent years, the signal simulation and control of the hand and tendon system have been the focus of scholars' research. Information measurement and acquisition require an observer, while feedback control of the system requires a controller to realize it [1–3]. The framework of control theory helps to understand the complex limb movements and regulatory mechanisms in the human neuromuscular system. The central nervous system receives input information through proprioceptors, which helps regulate and maintain the balance of human movement [4]. People can use key motion information observed by the observer to construct control models that simulate human movement processes. Although there are indeed differences between biological neural networks and artificial neural networks, such control strategies are useful in studying human motor control. In reference [5], a motion control model was proposed and evaluated through neuromechanical simulation, which consists of a controller and a musculoskeletal model, representing the central nervous system and the body.

The observer design problem for the nonlinear hybrid system has received more and more attention since the eighties [6–8]. High-gain observer is an important tool for studying sampling output feedback control of nonlinear systems [9–13]. In the

earlier time, Doyle and Steinjiang applied high-gain observers to the design of robust observers for linear systems [14]. The early work of high-gain observers in nonlinear systems began in the late 1880s [15,16], and after that, this technique has been applied to subsequent studies. Gauthier and other scholars devote themselves to the study of nonlinear systems under the condition of global Lipschitz to obtain the global results [17], the observer is constructed under the assumption that the conclusions obtained in this paper can be extended to a wider range of nonlinear systems. The observer is suitable for nonlinear systems and autonomous systems that can be observed by any input. Esfandiari and Khalil have proved that in the absence of the whole local Lipschitz condition, there will be a peak phenomenon, which will produce a similar pulse. Therefore, when the design of the observer gain is high enough, a high-gain observer may destroy the stability of closed-loop nonlinear hybrid systems [18].

The problem of information measurement noise and model uncertainties has attracted great attention from scholars [19,20]. In order to obtain accurate observation information, a switching gain observer is proposed in [21], because of modeling uncertainty, the authors construct a switched-gain observer to decrease the manifestations of the balance in the system states. The authors of [22] construct the observer gain based on the symmetric positive definite matrix with simple structure and try to find an algorithm that can calculate the state observer gain. The scholars have done in-depth research on high-gain observers in [23]. Based on the above discussion, to promote the results mentioned above, we try to consider uncertain nonlinear systems with sampled-data output measurements whose nonlinearity terms are unknown, and the nominal model of unmodeled dynamics satisfies weaker Lipschitz conditions. The conditions in this article about asynchronous sampling observation and control are suitable for a wider nonlinear system.

The main contributions of this article are two points. One is to allow the model to be uncertain; the condition in this paper is weaker than the classic Lipschitz condition; therefore, the conclusions obtained in this paper can be generalized to a wider range of nonlinear hybrid biomechanical systems. The unmodeled dynamics can be attenuated by increasing the gain. The other is that we consider the separation principle, the design of the asynchronous controller to realize the nervous system feedback control based on the state information observed by the high-gain observer.

The main contents of this paper are as follows: In section 2, materials and methods are given. The main result is in section 3. Discussion in section 4. Section 5 to illustrate the conclusion of this article.

2. Materials and methods

In order to better carry out the theoretical analysis, we propose the following lemma, which plays a key role in the main results of the study.

Lemma 1. [24]. For any matrix $U \in \mathbb{R}^{n \times n}$ it has the positive definite property, $a > 0$ and $b > 0$ are scalars, vector function $\phi: [a, b] \rightarrow \mathbb{R}^n$ such the integrations concerned are well defined, the following integral inequality holds:

$$\int_a^b \phi^T(s)U\phi(s)ds \geq \frac{1}{b-a} \int_a^b \phi^T(s)dsU \int_a^b \phi(s)ds.$$

Lemma 2. [25]. For constant matrices with appropriate dimensions S_1, S_{12}, S_{22} , where $S_1 = S_1^T > 0, S_2 = S_2^T > 0$ if $-S_1 + S_{12}S_2^{-1}S_{12}^T < 0$ and then the following inequality holds:

$$\begin{bmatrix} -S_1 & S_{12} \\ S_{12}^T & -S_2 \end{bmatrix} < 0.$$

3. Main result

3.1. Systems description and preliminaries

Consider the nonlinear hybrid biomechanical system proposed below:

$$\begin{cases} \dot{x}_i(t) = x_{i+1}(t) + f_i(x_1(t), \dots, x_i(t)), i = 1 \dots n - 1 \\ \dot{x}_n(t) = \varphi(w, x) + u(t) \\ y = x_1(t) \end{cases} \quad (1)$$

where $x(t) \in R^n$ is the state vector about the system above, $u(t) \in R$ represents input of controller, $y(t) \in R$ stands for measurement of the sensor output, $f_i(x_1 \dots x_i)$ is a nonlinear functions satisfying the conditions:

$$|f_i(x_1 \dots x_i) - f_i(\hat{x}_1 \dots \hat{x}_i)| \leq \sum_{j=1}^i l_j |x_j - \hat{x}_j| \quad (2)$$

where $l_i, i = 1, 2, \dots, n - 1$, are nonnegative constants, the unknown function with unmodeled dynamics $\varphi(w, x)$ satisfies global Lipschitz conditions. It's worth noting that the only thing that can be measured is the output $y(t) = x_1(t)$ from the analyzed hybrid system in discrete instant t_k , thus, according to obtained the sampled output $y(t_k)$ that was obtained at discrete time, a state observer with sampled and corresponded to system (1) is proposed as follows:

$$\begin{cases} \dot{\hat{x}}_i(t) = \hat{x}_{i+1}(t) + f_i(\hat{x}_1(t), \dots, \hat{x}_i(t)) + \frac{\alpha_i}{\varepsilon^i} (y(t_k) - \hat{x}_1(t_k)), i = 1 \dots n - 1, t \in \\ \dot{\hat{x}}_n(t) = \varphi_0(\hat{x}) + \frac{\alpha_n}{\varepsilon^n} (y(t_k) - \hat{x}_1(t_k)) + u(t), \end{cases} \quad (3)$$

where $\hat{x}(t) \in R^n$ is the observer state, $\varphi_0(\hat{x}) = 0$ is a nominal model of $\varphi(w, x)$ satisfy the conditions

$$|\varphi(w, x) - \varphi_0(z)| \leq L \|x - z\| + M \quad (4)$$

where $L > 0, M > 0$ are constants.

In order to suppress and reduce the influence of unmodeled dynamics, a controller based on a sample-and-hold Luenberger observer is designed as follows:

$$\begin{cases} \dot{\hat{x}}_i(t) = \hat{x}_{i+1}(t) + f_i(\hat{x}_1(t), \dots, \hat{x}_i(t)) + \frac{\alpha_i}{\varepsilon^i} (x_1(t_k) - \hat{x}_1(t_k)), t \in [t_k, t_{k+1}) \\ \dot{\hat{x}}_n(t) = \varphi_0(\hat{x}) + \frac{\alpha_n}{\varepsilon^n} (x_1(t_k) - \hat{x}_1(t_k)) + u(t) \\ u(t) = -\sum_{j=1}^n \frac{\alpha_j}{\varepsilon^j} k_{n+1-j} \hat{x}_{n+1-j}(s_{\bar{k}}), t \in [s_{\bar{k}}, s_{\bar{k}+1}), \end{cases} \quad (5)$$

where $i = 1 \dots n - 1$, the time sequences $\{t_k\}$ and $\{s_{\bar{k}}\}$ are not any strictly increasing but also satisfy the following constraints:

$$t_0 = 0, \bar{h}_{10} \leq t_{k+1} - t_k \leq \bar{h}_1,$$

$$s_0 = 0, \bar{h}_{20} \leq s_{\bar{k}+1} - s_{\bar{k}} \leq \bar{h}_2, k \in \mathbb{N}.$$

where $\bar{h}_{10}, \bar{h}_1, \bar{h}_{20}, \bar{h}_2$ are positive definite scalars. In addition, for the sake of later analysis, we introduce the following notation:

$$\psi(t) = t_{k+1} - t, \rho(t) = t - t_k, t \in [t_k, t_{k+1}),$$

$$\tilde{\psi}(t) = s_{\bar{k}+1} - t, \tilde{\rho}(t) = t - s_{\bar{k}}, t \in [s_{\bar{k}}, s_{\bar{k}+1}),$$

$$I_1 = [I_n \ 0_n], I_2 = [0_n \ I_n], I_3 = [I_n \ -I_n].$$

By setting $e(t) = x(t) - \hat{x}(t)$ the error dynamics (3) can be converted and represented in the following form:

$$\begin{cases} \dot{e}_i(t) = -\frac{\alpha_i}{\varepsilon^i} e_1(t_k) + f_i(x_1(t), \dots, x_i(t)) - f_i(\hat{x}_1(t), \dots, \hat{x}_i(t)) + e_{i+1}(t) \\ \dot{e}_n(t) = -\frac{\alpha_n}{\varepsilon^n} e_1(t_k) + \phi(w, x) - \phi_0(\hat{x}), \end{cases} \quad (6)$$

where the value of $e_i(t)$ are equal to $x_i(t) - \hat{x}_i(t)$. In order to simplify the analysis in subsequent research, coordinate transformation is made as follows

$$\gamma_i(t) = \frac{x_i(t) - \hat{x}_i(t)}{\varepsilon^{n-i}} \quad (7)$$

$$\delta_i(t) = \frac{f_i(x_1(t), \dots, x_i(t)) - f_i(\hat{x}_1(t), \dots, \hat{x}_i(t))}{\varepsilon^{n-i}}, \delta_n(t) = \phi(w, x) - \phi_0(x) \quad (8)$$

where $i = 1, \dots, n - 1$, therefore, the system (6) and the following system form are equivalent,

$$\begin{aligned} \varepsilon \dot{\gamma}_i(t) &= \alpha_i(\gamma_1(t) - \gamma_1(t_k)) - \alpha_i \gamma_1(t) + \gamma_{i+1}(t) + \varepsilon \delta_i(t) \quad i = 1, \dots, n - 1, \\ \varepsilon \dot{\gamma}_n(t) &= \alpha_n(\gamma_1(t) - \gamma_1(t_k)) - \alpha_n \gamma_1(t) + \varepsilon \delta_n(t). \end{aligned} \quad (9)$$

In order to better analyze the system (9), we introduce the following symbols

$$\varepsilon \dot{\gamma}(t) = \varepsilon \delta(t) + Ar(t) + \bar{\alpha}(\gamma_1(t) - \gamma_1(t_k)) \quad (10)$$

$$\varepsilon \dot{\gamma}(t) = A_\xi(t) \xi(t) \quad (11)$$

where

$$A = \begin{bmatrix} -\alpha_1 & 1 & 0 & \dots & 0 & 0 \\ -\alpha_2 & 0 & 1 & \dots & 0 & 0 \\ \vdots & \vdots & \vdots & \vdots & \vdots & \vdots \\ -\alpha_{n-1} & 0 & 0 & \dots & 0 & 1 \\ -\alpha_n & 0 & 0 & \dots & 0 & 0 \end{bmatrix},$$

$$\gamma(t) = [\gamma_1(t) \ \dots \ \gamma_n(t)]^T, \delta(t) = [\delta_1(t) \ \dots \ \delta_n(t)]^T,$$

$$\bar{\alpha} = [\alpha_1 \ \dots \ \alpha_n]^T, \bar{I}_1 = [1 \ \dots \ 0]_{1 \times n}, \bar{A} = [A \ \bar{\alpha} \bar{I}_1],$$

$$\eta(t) = [\gamma(t) \ \tilde{\gamma}(t)]^T, \xi(t) = [\eta(t) \ \varepsilon \delta(t)]^T, A_\xi = [\bar{A} \ I], \tilde{\gamma}(t) = \gamma(t) - \gamma(t_k).$$

Therefore, the stability problem of the error system (6) can be transformed into the stability problem of the system (9). According to Equations (2) – (4) and Equations (8) – (9), we have

$$|\delta(t)| \leq \bar{L}\|\gamma(t)\| + \bar{M} \quad (12)$$

3.2. the stability of error system

In this section, we will use convex combination techniques and the Lyapunov method to solve the stabilization for the error system problem of system (9).

Theorem 1. consider the system of (9), assume the conditions of (2) and (4) are established, given $\alpha_1 > 0$, if there exist matrices $P_1 > 0, R_1 > 0$ which dimensions are all $n \times n$, the matrix M_1 has dimensions $2n \times n$, $n \times n$ matrices $X_1 = X_1^T, X_2 > 0$, scalars $\beta_1, \beta_0, L, M > 0$, such that the LMIs satisfy the following form:

$$\begin{bmatrix} \Phi(t) + \Pi(t) & \Omega(t) & \bar{h}_1 \bar{A}^T R_1 \\ * & -\beta_0 I & \bar{h}_1 I^T R_1 \\ * & * & -\bar{h}_1 R_1 \end{bmatrix} < 0 \quad (13)$$

$$\begin{bmatrix} \Phi(t) + \Pi(t) & \Omega(t) & \bar{h}_1 \bar{A}^T R & \bar{h}_1 M_1 e^{\alpha_1 \bar{h}_1} \\ * & -\beta_0 I & \bar{h}_1 R_1 & 0 \\ * & * & -\bar{h}_1 R_1 & 0 \\ * & * & * & -\bar{h}_1 R_1 \end{bmatrix} < 0 \quad (14)$$

where

$$\begin{aligned} \Phi(t) &= 2\varepsilon\alpha_1 I_1^T P_1 I_1 + (2\varepsilon\alpha_1 \bar{h}_1 - \varepsilon) I_2^T X_1 I_2 + (4\varepsilon\alpha_1 \bar{h}_1 - 2\varepsilon) I_3^T X_2 I_2 + \varepsilon^2 L^2 (1 + \beta_1) \beta_0 I_1^T I_1 + 2\bar{h}_1 I_2^T X_1 \bar{A} + \\ & 4\bar{h}_1 I_3^T X_2 \bar{A}, \Pi(t) = I_1^T P_1 \bar{A} + \bar{A}^T P_1 I_1 + \varepsilon M_1 I_2 + \varepsilon I_2^T M_1^T, \Omega(t) = I_1^T P_1 + \bar{h}_1 I_2^T X_1 + 2\bar{h}_1 I_3^T X_2. \end{aligned}$$

Then, for some constants a, b, c they are all satisfied with the positive definiteness condition and ε , with $\varepsilon \ll 1$ such that the solution from γ_0 is satisfied as follows estimates:

$$\|\gamma(t)\| \leq a\|\gamma(t_0)\|e^{-bt} + \varepsilon^{\frac{1}{2}}Mc \quad (15)$$

Proof of Theorem 1. In order to carry out the stability analysis of system (9), we introduce the following Lyapunov functional:

$$\begin{aligned} V(t) &= \gamma^T(t)\varepsilon P_1 \gamma(t) + \varepsilon^2 \psi(t) \int_{t-\rho(t)}^t e^{2\alpha_1(s-t)} \dot{\gamma}^T(s) R_1 \dot{\gamma}(s) ds + \varepsilon \psi(t) (\tilde{\gamma}^T(t) X_1 \tilde{\gamma}(t) + 2(\gamma(t) \\ & - \tilde{\gamma}(t))^T X_2 \tilde{\gamma}(t)) \end{aligned} \quad (16)$$

We can deduce that the time derivative of $V(t)$ along the trajectory of (9) is given by

$$\begin{aligned} \dot{V}(t) &= 2\gamma^T(t)P_1\varepsilon\dot{\gamma}(t) - \varepsilon^2 \int_{t-\rho(t)}^t \dot{\gamma}^T(s)e^{2\alpha_1(s-t)}R_1\dot{\gamma}(s)ds + \dot{\gamma}^T(t)\psi(t)\varepsilon^2R_1\dot{\gamma}(t) \\ & - 2\varepsilon^2\alpha_1\psi(t) \int_{t-\rho(t)}^t \dot{\gamma}^T(s)e^{2\alpha_1(s-t)}R_1\dot{\gamma}(s)ds - \varepsilon[\tilde{\gamma}^T(t)X_1\tilde{\gamma}(t) + 2(\gamma(t) - \tilde{\gamma}(t))^T X_2 \tilde{\gamma}(t)] \\ & + 2\psi(t)\tilde{\gamma}(t)X_1\varepsilon\dot{\gamma}(t) + 2\psi(t)(\gamma(t) - \tilde{\gamma}(t))^T X_2 \varepsilon\dot{\gamma}(t) \end{aligned} \quad (17)$$

Considering (16) we obtain:

$$-2 \int_{t-\rho(t)}^t \dot{\gamma}^T(s) \varepsilon^2 \alpha_1 \psi(t) e^{2\alpha_1(s-t)} R_1 \dot{\gamma}(s) ds = 2\gamma^T(t) \varepsilon \alpha_1 P_1 \gamma(t) + 2\varepsilon \psi(t) \alpha_1 (\tilde{\gamma}^T(t) X_1 \tilde{\gamma}(t) + 2(\gamma(t) - \tilde{\gamma}(t))^T X_2 \tilde{\gamma}(t)) - 2\alpha_1 V(t).$$

Considering $\tilde{\gamma}(t)$ can be expressed equivalently as $\int_{t-\rho(t)}^t \dot{\gamma}(s) ds$. Therefore, the following relationship is reasonable:

$$\begin{aligned} 0 &= 2\eta^T(t) \varepsilon M_1 (\tilde{\gamma}(t) - \int_{t-\rho(t)}^t \dot{\gamma}(s) ds) \\ &\leq \eta^T(t) (\varepsilon M_1 I_2 + \varepsilon I_2^T M_1^T) \eta(t) + \bar{h}_1 \eta^T(t) M_1 R_1^{-1} e^{2\alpha_1 \bar{h}_1} M_1^T \eta(t) \\ &+ \int_{t-\rho(t)}^t \dot{\gamma}^T(s) \varepsilon^2 R_1 e^{2\alpha_1(s-t)} \dot{\gamma}(s) ds \end{aligned} \quad (18)$$

Form Equation (12), one can deduce that

$$0 \leq \varepsilon^2 (L^2 (1 + \beta_1) \gamma^T(t) \gamma(t) + M^2 (1 + \frac{1}{\beta_1}) \|\delta(t)\|^2) \beta_0 \quad (19)$$

where $\beta_1 > 0, \beta_0 > 0$, for $t \in [t_k, t_{k+1})$, combine (17), (18) with (19), we obtain that

$$\dot{V}(t) \leq -2\alpha_1 V(t) + \varepsilon^2 \beta_0 M^2 (1 + \frac{1}{\beta_1}).$$

Further,

$$\|\gamma(t)\| \leq \sqrt{\frac{\lambda_2}{\lambda_1}} e^{-\alpha_1 t} \|\gamma(t_0)\| + \sqrt{\frac{1}{\lambda_1} \frac{1}{2\alpha_1} (1 + \frac{1}{\beta_0} \beta_1) \varepsilon M} \quad (20)$$

where $\lambda_1 = \lambda_{\min}(P_1), \lambda_2 = \lambda_{\max}(P_1)$. Therefore, we can obtain (15), where the $\varepsilon > 0, \varepsilon \ll 1$.

The proof is completed. \square

3.3. Feedback control based on high-gain observer

In this section, we will implement asynchronous feedback control of the system. To achieve robust stabilization of the system (1) based on the high-gain observer obtained from previous research, we first perform the following transformation:

$$\vartheta_i = \frac{x_i}{\varepsilon^{n-i}}, i = 1 \dots n, \tilde{\delta}_i = \frac{f(x_1(t), \dots, x_i(t))}{\varepsilon^{n-i}}, i = 1 \dots n-1, \tilde{\delta}_n = \frac{\phi(w, x)}{\varepsilon^0} \quad (21)$$

Substituting the controller designed (5) into (1), we have

$$\begin{cases} \dot{x}_i(t) = x_{i+1}(t) + f_i(x_1(t), \dots, x_i(t)), \\ \dot{x}_n(t) = - \sum_{i=1}^n \frac{\alpha_i}{\varepsilon^i} k_{n+1-i} x_{n+1-i}(s_{\bar{k}}) + \phi(w, x) + \sum_{i=1}^n \frac{\alpha_i}{\varepsilon^i} k_{n+1-i} e_{n+1-i}(s_{\bar{k}}), \end{cases} \quad (22)$$

where $i = 1 \dots n-1$, coordinate transformation (22) can be converted to closed-loop system (23) into the following form

$$\begin{cases} \varepsilon \dot{\vartheta}_i(t) = \vartheta_{i+1}(t) + \varepsilon \cdot \frac{f_i(x_1(t) \cdots x_i(t))}{\varepsilon^{n-i}}, i = 1 \cdots n - 1 \\ \varepsilon \dot{\vartheta}_n(t) = \sum_{i=1}^n -\alpha_i k_{n+1-i} \vartheta_{n+1-i}(t) + \sum_{i=1}^n \alpha_i k_{n+1-i} (\vartheta_{n+1-i}(t) - \vartheta_{(n+1-i)}(s_{\bar{k}})) \\ + \sum_{i=1}^n \alpha_i k_{n+1-i} \gamma_{n+1-i}(s_{\bar{k}}) + \phi(w, x), \end{cases} \quad (23)$$

Therefore, we can obtain the form below

$$\varepsilon \dot{\vartheta}(t) = B\vartheta(t) + \tilde{K}\tilde{\vartheta}(t) + \varepsilon\tilde{\delta}(t) + \tilde{K}\gamma(s_{\bar{k}}) = B_k\zeta(t) \quad (24)$$

where $B_k = [\tilde{B} \quad I \quad \tilde{K}]$, $\tilde{B} = [B \quad \tilde{K}]$.

$$B = \begin{bmatrix} 0 & 1 & \cdots & 0 & 0 \\ 0 & 0 & \cdots & 0 & 0 \\ \vdots & \vdots & \vdots & \vdots & \vdots \\ 0 & 0 & \cdots & 0 & 1 \\ -\alpha_n k_1 & -\alpha_{n-1} k_2 & \cdots & -\alpha_2 k_{n-1} & -\alpha_1 k_n \end{bmatrix},$$

$$\tilde{K} = \begin{bmatrix} 0 & 0 & 0 & \cdots & 0 & 0 \\ 0 & 0 & 0 & \cdots & 0 & 0 \\ \vdots & \vdots & \vdots & \vdots & \vdots & \vdots \\ 0 & 0 & 0 & \cdots & 0 & 0 \\ \alpha_n k_1 & \alpha_{n-1} k_2 & \alpha_{n-2} k_3 & \cdots & \alpha_2 k_{n-1} & \alpha_1 k_n \end{bmatrix},$$

$$\tilde{\vartheta}(t) = [\vartheta_1(t) - \vartheta_1(s_{\bar{k}}) \quad \cdots \quad \vartheta_n(t) - \vartheta_n(s_{\bar{k}})]^T, \vartheta(t) = [\vartheta_1(t) \quad \cdots \quad \vartheta_n(t)]^T,$$

$$\gamma(s_{\bar{k}}) = [\gamma_1(s_{\bar{k}}) \quad \cdots \quad \gamma_i(s_{\bar{k}}) \quad \cdots \quad \gamma_n(s_{\bar{k}})]^T,$$

$$\varepsilon \tilde{\delta} = \varepsilon \left[\frac{f_1(x_1(t))}{\varepsilon^{n-1}} \quad \cdots \quad \frac{f_{n-1}(x_1(t) \cdots x_{n-1}(t))}{\varepsilon^1} \quad \frac{\phi(w, x)}{\varepsilon^0} \right]^T,$$

$$\zeta(t) = [\zeta_0(t) \quad \varepsilon \tilde{\delta} \quad \gamma(s_{\bar{k}})]^T, \zeta_0(t) = [\vartheta(t) \quad \tilde{\vartheta}(t)]^T.$$

Theorem 2. Consider the system of (24), given $\alpha_2 > 0$, if there exist matrices with dimension $n \times n$, $P_2 > 0$, $2n \times n$ matrices $M_2 > 0$, matrices $R_2 > 0$ which has dimension $n \times n$, $n \times n$ matrices $\tilde{X}_1 = \tilde{X}_1^T$, \tilde{X}_2 and scalars $\tilde{\beta}_0 > 0, \gamma_0 > 0, \tilde{M} > 0$, such that the following LMIs are satisfied,

$$\mathcal{E}_1 = \begin{bmatrix} \Theta(t) + \Upsilon(t) & \Psi(t) & \bar{h}_2 \bar{B}^T R_2 \\ * & -\tilde{\beta}_0 I & \bar{h}_2 I^T R_2 \\ * & * & -\bar{h}_2 R_2 \end{bmatrix} < 0 \quad (25)$$

$$\mathcal{E}_2 = \begin{bmatrix} \Theta(t) + \Upsilon(t) & \Psi(t) & \bar{h}_2 M_2 e^{\alpha_2 \bar{h}_2} \\ * & -\tilde{\beta}_0 I & 0 \\ * & * & -\bar{h}_2 R_2 \end{bmatrix} < 0 \quad (26)$$

where $\Theta(t) = I_1^T P_2 \tilde{B} + \tilde{B}^T P_2 I_1 + \varepsilon M_2 I_2 + \varepsilon I_2^T M_2^T, I_1, I_2, I_3$ are Same as before descriptions.

$$\Upsilon(t) = 2\alpha_2 \varepsilon I_1^T P_2 I_1 + (2\alpha_2 \bar{h}_2 \varepsilon - \varepsilon) I_2^T \tilde{X}_1 I_2 + (4\alpha_2 \bar{h}_2 \varepsilon - 2\varepsilon) I_3^T \tilde{X}_2 I_2 + 2\bar{h}_2 I_2^T \tilde{X}_1 \tilde{B} + 2\bar{h}_2 I_3^T \tilde{X}_2 \tilde{B} + \bar{L}^2 (1 + \tilde{\beta}) \varepsilon^2 \tilde{\beta}_0 \quad \Psi(t) = I_1^T P_2 I + \bar{h}_2 I_2^T \tilde{X}_1 I + \bar{h} I_3^T \tilde{X}_2 I.$$

Then system (24) is stable.

Proof of Theorem 2. We introduce the following Lyapunov functional.

$$V(t) = 2(\vartheta(t) - \tilde{\vartheta}(t))^T \bar{X}_2 \tilde{\vartheta}(t) + \vartheta^T(t) \varepsilon P_2 \vartheta(t) + \varepsilon^2 \tilde{\psi}(t) \int_{t-\tilde{\rho}(t)}^t \dot{\vartheta}^T(s) e^{2\alpha_2(s-t)} R_2 \dot{\vartheta}(s) ds + \varepsilon \tilde{\psi}(t) (\tilde{\vartheta}^T(t) \bar{X}_1 \tilde{\vartheta}(t)) \quad (27)$$

$$\begin{aligned} \dot{V}(t) = & 2\varepsilon \vartheta^T(t) (t) P_2 \dot{\vartheta}(t) - \varepsilon^2 \int_{t-\tilde{\rho}(t)}^t \dot{\vartheta}^T(s) e^{2\alpha_2(s-t)} R_2 \dot{\vartheta}(s) ds + \dot{\vartheta}(t) \varepsilon^2 h \tilde{\psi}(t) R_2 \dot{\vartheta}(t) \\ & - 2\alpha_2 \psi(t) \varepsilon^2 \int_{t-\tilde{\rho}(t)}^t \dot{\vartheta}^T(s) e^{2\alpha_2(s-t)} R_2 \dot{\vartheta}(s) ds - \varepsilon [2(\vartheta(t) - \tilde{\vartheta}(t))^T \bar{X}_2 \tilde{\vartheta}(t) + \tilde{\vartheta}^T(t) \bar{X}_1 \tilde{\vartheta}(t)] \\ & + 2\tilde{\psi}(t) \tilde{\vartheta}^T(t) \bar{X}_1 \varepsilon \dot{\vartheta}(t) + 4\tilde{\psi}(t) (\vartheta(t) - \tilde{\vartheta}(t))^T \bar{X}_2 \varepsilon \dot{\vartheta}(t) \end{aligned} \quad (28)$$

set

$$\Xi(t) = \begin{bmatrix} \mu \Xi_1 + (1 - \mu) \Xi_2 & \Psi(t) \\ * & -\tilde{\beta}_0 I \end{bmatrix}$$

where $\mu \in (0,1)$ in view of Schur complement, from (25) and (26), we have

$$\tilde{\Xi} = \begin{bmatrix} \Xi(t) & \tilde{\Psi}(t) \tilde{K} \\ * & \tilde{K}^T R \tilde{K} - \gamma_0 I \end{bmatrix} < 0 \quad (29)$$

$$\tilde{\Psi}(t) = \begin{bmatrix} I_1^T \\ 0 \\ 0 \end{bmatrix} P_2 + \tilde{h}_2 \begin{bmatrix} B^T \\ I^T \\ 0 \end{bmatrix} R_2 + \tilde{h}_2 \begin{bmatrix} I_2^T \\ 0 \\ 0 \end{bmatrix} \bar{X}_1 + \tilde{h}_2 \begin{bmatrix} I_3^T \\ 0 \\ 0 \end{bmatrix} \bar{X}_2. \quad (30)$$

From (30), it follows that

$$\dot{V} \leq -2\alpha_2 V(t) + \gamma_0^2 \|\gamma(s_{\bar{k}})\|^2 + \tilde{M}^2 (1 + \frac{1}{\tilde{\beta}}) \varepsilon^2 \tilde{\beta}_0,$$

From **Theorem 1**, we can obtain that there exists a scalar $\bar{a} > 0$ such that the following inequality holds $\|\vartheta(t)\|^2 \leq \bar{a}^2 \|\vartheta(0)\|^2 e^{-2\alpha_2 t} + o(\varepsilon), \forall t \geq 0$, where $\bar{a} = \sqrt{\frac{\lambda_{P_2 \max}}{\lambda_{P_2 \min}}}$.

When ε is arbitrary small, the sampled-data control strategy based on a high-gain sampled-data observer realizes the robust stabilization of the closed-loop system. \square

3.4. A numerical example

In the next part, we illustrate effectiveness with a numerical example about the developed methodology. First, we consider the below proposed nonlinear biomechanical system.

$$\begin{cases} \dot{x}_1 = x_2(t) \\ \dot{x}_2 = -\frac{F_2(t)}{J_2} x_2(t) - \frac{K}{J_2} x_1(t) - \frac{mgd}{J_2} (\cos(x_1(t)) - 1) + x_3(t) \\ \dot{x}_3 = x_4(t) \\ \dot{x}_4 = \frac{K^2}{N^2 J_1 J_2} x_1(t) - \frac{K}{N J_2} x_3(t) - \frac{F_1(t)}{J_1} x_4(t) + \frac{1}{10} (|x_3(t) + 1| - |x_3(t) - 1|) + u(t) \\ y(t_k) = x_1(t_k), \end{cases} \quad (30)$$

According to the previous observer design method, in order to achieve system stability, we construct a feedback controller with discrete time output

$$\begin{cases} \dot{\hat{x}}_1 = \frac{a_1}{\varepsilon} (y(t_k) - \hat{x}_1(t_k)) + \hat{x}_2(t), t \in [t_k, t_{k+1}) \\ \dot{\hat{x}}_2 = \frac{a_2}{\varepsilon^2} (y(t_k) - \hat{x}_1(t_k)) + \hat{x}_3(t) - \frac{K}{J_2} \hat{x}_1(t) - \frac{F_2(t)}{J_2} \hat{x}_2(t) - \frac{mgd}{J_2} (\cos(\hat{x}_1(t)) - 1) \\ \dot{\hat{x}}_3 = \frac{a_3}{\varepsilon^3} (y(t_k) - \hat{x}_1(t_k)) + \hat{x}_4(t) \\ \dot{\hat{x}}_4 = \frac{a_4}{\varepsilon^4} (y(t_k) - \hat{x}_1(t_k)) + \frac{K^2}{J_1 J_2 N^2} \hat{x}_1(t) - \frac{K}{J_2 N} \hat{x}_3(t) - \frac{F_1(t)}{J_1} x_4(t) + \frac{1}{10} (|\hat{x}_3(t) + 1| - |\hat{x}_3(t) - 1|) \\ + u(t) \\ u(t) = -[k_1 \frac{a_4}{\varepsilon^4} \hat{x}_1(s_{\bar{k}}) + k_2 \frac{a_3}{\varepsilon^3} \hat{x}_2(s_{\bar{k}}) + k_3 \frac{a_2}{\varepsilon^2} \hat{x}_3(s_{\bar{k}}) + k_4 \frac{a_1}{\varepsilon} \hat{x}_4(s_{\bar{k}})], t \in [s_{\bar{k}}, s_{\bar{k}+1}), \end{cases} \quad (31)$$

System parameters $K/(J_2 N) = 3$, $K^2/(J_1 J_2 N^2) = 2$, $mgd/J_2 = 4$, $K/J_2 = 5$.

$F_2(t)/J_2 = 10$, $F_1(t)/J_1 = 10$, We set the value of controller gain k_1, k_2, k_3, k_4 and the observer gain of the representative about a_1, a_2, a_3, a_4 are 40, 78, 49, 12, 4, 6, 4, 1 respectively. The value $x_1(0) = -5$, $x_2(0) = -1$, $x_3(0) = 4$, $x_4(0) = 20$ takes the form.

Initial estimate $\hat{x}_1(0) = 5$, $\hat{x}_2(0) = 3$, $\hat{x}_3(0) = -1$, $\hat{x}_4(0) = -4$ With the choice of value about $\varepsilon = 0.41$, the actuator sampling $\{s_{\bar{k}}\}$ and the sensor sampling $\{t_k\}$ are randomly generated, $\bar{h}_1 = 0.003$, $\bar{h}_2 = 0.003$. The numerical simulation results are as follows for **Figure 1–3**.

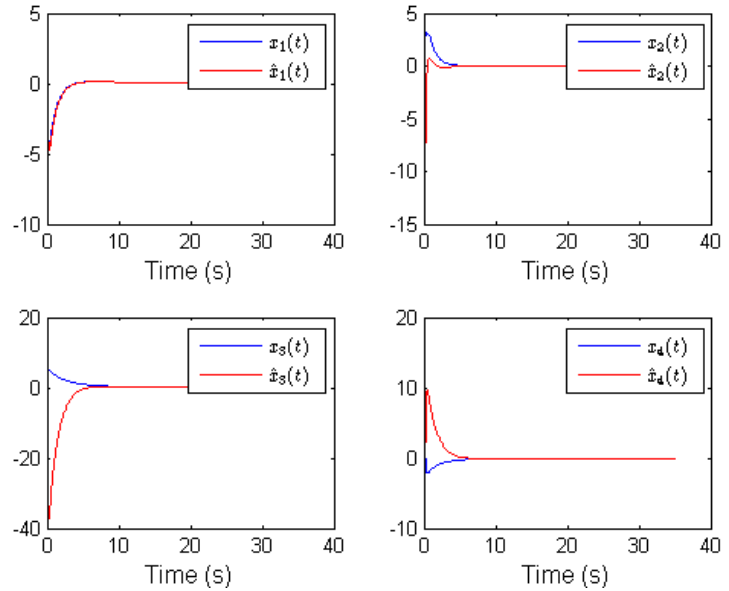


Figure 1. The simulation results: $x(t)$ and its estimate $\hat{x}(t)$.

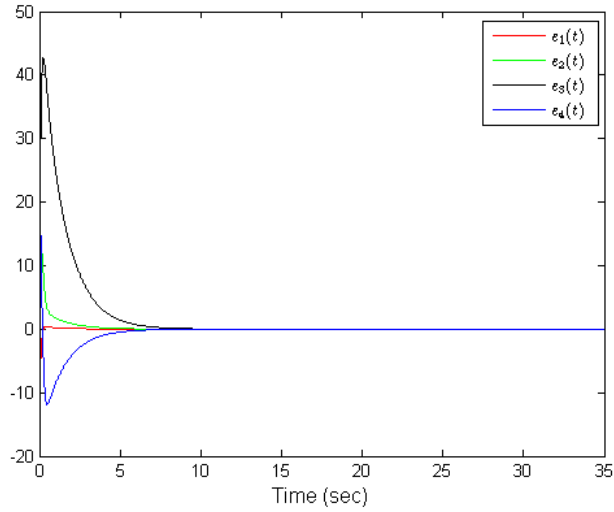


Figure 2. The simulation results of $e(t)$.

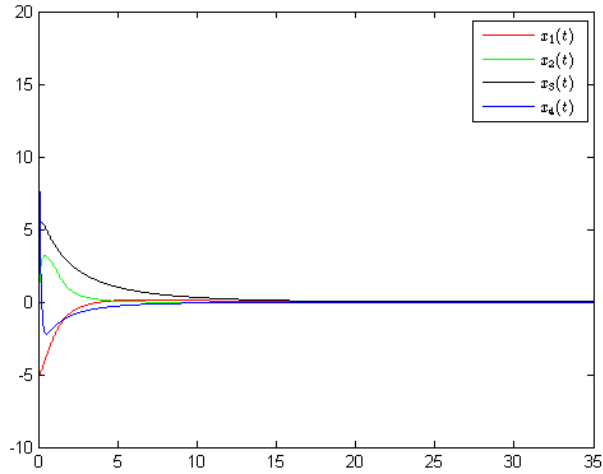


Figure 3. The simulation results of $x(t)$.

4. Discussion

Remark 1. Noting that $\gamma_i(t) = e_i(t)/\varepsilon^{n-i}$, the $\|\gamma(t)\|$ can be estimated implies $e(t)$ can be estimated. Therefore,

$$\|\gamma(t)\| = \frac{1}{\varepsilon^{n-1}} \sqrt{e_1^2(t) + \varepsilon^2 e_2^2(t) + \dots + (\varepsilon^{n-1})^2 e_n^2(t)} \leq \frac{1}{\varepsilon^{n-1}} \|e(t)\|,$$

$$\|\gamma(t)\| \leq a \|\gamma(t_0)\| e^{-bt} + \varepsilon^{\frac{1}{2}} Mc \leq \frac{1}{\varepsilon^{n-1}} a e^{-bt} \|e(0)\| + \varepsilon^{\frac{1}{2}} Mc.$$

Which shows that

$$\|e_i(t)\| \leq \frac{1}{\varepsilon^{i-1}} a e^{-bt} \|e(0)\| + \varepsilon^{n-(i-\frac{1}{2})} Mc \quad (32)$$

For all $t \geq 0$. Hence, $\|e_i(t)\|$ decay exponentially fast and are ultimately bounded.

Remark 2. Noting that $\vartheta_i(t)$ is obtained from $x_i(t)$ Through the coordinate transformation mentioned earlier $\vartheta_i(t) = x_i(t)/\varepsilon^{n-i}$, the $\vartheta_i(t)$ can be estimated implies $x_i(t)$ can be estimated. Therefore,

$$\|\vartheta(t)\| = \frac{1}{\varepsilon^{n-1}} \sqrt{\sum_{i=1}^n x_i^2 (\varepsilon^{i-1})^2} \leq \frac{1}{\varepsilon^{n-1}} \|x(t)\|,$$

$$\|\vartheta(t)\| \leq \bar{a} \|\vartheta(0)\| e^{-\alpha_2 t} + o(\varepsilon) \leq \bar{a} e^{-\alpha_2 t} \frac{1}{\varepsilon^{n-1}} \|x(0)\| + o(\varepsilon).$$

Which shows that

$$\|x_i(t)\| \leq \frac{1}{\varepsilon^{i-1}} \bar{a} e^{-\alpha_2 t} \|x(0)\| + o(\varepsilon) \quad (33)$$

For all $t \geq 0$. Hence, $\|x_i(t)\|$ decay exponentially fast and are ultimately bounded.

5. Conclusion

In life, human beings perform various action tasks. The central nervous system coordinates all aspects of body movements through control to ensure successful execution [26–30]. In this article, we presented a high-gain observer-based controller for modeling the movement of biomechanical limbs. Our controller model reconstructs movement information data with unmodeled dynamics and nonlinear dynamics. It is beneficial to regulate and maintain the balance of human movement. Firstly, a discrete time sampling high-gain observer is proposed for a class of biomechanical systems with unmodeled dynamics. Then, a Lyapunov function has been introduced to deeply analyze the stability of the composite system; the new condition is expressed by solving LMIs (linear matrix inequality). The asynchronous controller for the separation principle is designed to realize the nervous feedback system control based on the sampling discrete time high-gain observer. Finally, the last numerical example illustrates the feasibility and effectiveness of the results presented in this paper.

Author contributions: Conceptualization, LC and NY; methodology, LC; software, NY; validation, LC and NY; formal analysis, LC; investigation, NY; resources, LC; data curation, LC; writing—original draft preparation, LC; writing—review and editing, NY; visualization, LC; supervision, NY; project administration, LC; funding acquisition, LC. All authors have read and agreed to the published version of the manuscript.

Funding: Supported by Research Program of Chongqing University of Education (Grant No. KY202310C) and the Chongqing University of Education Smart Education Big Data Research Center

Ethical approval: Not applicable.

Conflict of interest: The authors declare no conflict of interest.

References

1. Andersen MS, Damsgaard M, Rasmussen J. Kinematic analysis of over-determinate biomechanical systems. *Computer Methods in Biomechanics and Biomedical Engineering*. 2009; 12(4): 371-384. doi: 10.1080/10255840802459412
2. Sachdeva P, Sueda S, Bradley S, et al. Biomechanical simulation and control of hands and tendinous systems. *ACM Transactions on Graphics*. 2015; 34(4): 1-10. doi: 10.1145/2766987
3. Hribernik M, Umek A, Tomažič S, et al. Review of Real-Time Biomechanical Feedback Systems in Sport and Rehabilitation. *Sensors*. 2022; 22(8): 3006. doi: 10.3390/s22083006

4. Siriphorn A, Chamonchant D, Boonyong S. The effects of vision on sit-to-stand movement. *Journal of Physical Therapy Science*. 2015; 27(1): 83-86. doi: 10.1589/jpts.27.83
5. Song S, Kidziński Ł, Peng XB, et al. Deep reinforcement learning for modeling human locomotion control in neuromechanical simulation. *Journal of NeuroEngineering and Rehabilitation*. 2021; 18(1). doi: 10.1186/s12984-021-00919-y
6. Thau FE. Observing the state of non-linear dynamic systems. *International Journal of Control*. 1973; 17(3): 471-479. doi: 10.1080/00207177308932395
7. Chen WH. Nonlinear Disturbance Observer-Enhanced Dynamic Inversion Control of Missiles. *Journal of Guidance, Control, and Dynamics*. 2003; 26(1): 161-166. doi: 10.2514/2.5027
8. Xiao W, Cao L, Li H, et al. Observer-based adaptive consensus control for nonlinear multi-agent systems with time-delay. *Science China Information Sciences*. 2020; 63(3). doi: 10.1007/s11432-019-2678-2
9. Abdel-Rahim O, Wang H. A New High Gain DC-DC Converter With Model-Predictive-Control Based MPPT Technique for Photovoltaic Systems. *CPSS Transactions on Power Electronics and Applications*. 2020; 5(2): 191-200. doi: 10.24295/cpsstpea.2020.00016
10. Zhang C, Wang C, Wang J, et al. Neuro-adaptive trajectory tracking control of underactuated autonomous surface vehicles with high-gain observer. *Applied Ocean Research*. 2020; 97: 102051. doi: 10.1016/j.apor.2020.102051
11. Zou D, Chen T, He W, et al. Observation of hybrid higher-order skin-topological effect in non-Hermitian topoelectrical circuits. *Nature Communications*. 2021; 12(1). doi: 10.1038/s41467-021-26414-5
12. Azizkhani M, Godage IS, Chen Y. Dynamic Control of Soft Robotic Arm: A Simulation Study. *IEEE Robotics and Automation Letters*. 2022; 7(2): 3584-3591. doi: 10.1109/lra.2022.3148437
13. Khalil HK. Cascade high-gain observers in output feedback control. *Automatica*. 2017; 80: 110-118. doi: 10.1016/j.automatica.2017.02.031
14. Doyle J, Stein G. Robustness with observers. *IEEE Transactions on Automatic Control*. 1979; 24(4): 607-611. doi: 10.1109/tac.1979.1102095
15. Esfandiari F, Khalil HK. Observer-based Control of Uncertain Linear Systems: Recovering State Feedback Robustness Under Matching Condition. In: *Proceedings of the 1989 American Control Conference*; 1989.
16. Kim BK, Chung WK. Advanced disturbance observer design for mechanical positioning systems. *IEEE Transactions on Industrial Electronics*. 2003; 50(6): 1207-1216. doi: 10.1109/tie.2003.819695
17. Gauthier JP, Hammouri H, Othman S. Simple observer for nonlinear systems applications to bioreactors. *IEEE Transactions on Automatic Control*. 1992; 37(6): 875-880. doi: 10.1109/9.256352
18. Esfandiari F, Khalil HK. Output feedback stabilization of fully linearizable systems. *International Journal of Control*. 1992; 56(5): 1007-1037. doi: 10.1080/00207179208934355
19. Tréangle C, Farza M, M'Saad M. Filtered high gain observer for a class of uncertain nonlinear systems with sampled outputs. *Automatica*. 2019; 101: 197-206. doi: 10.1016/j.automatica.2018.12.002
20. Chang Y, Zhang S, Alotaibi ND, et al. Observer-Based Adaptive Finite-Time Tracking Control for a Class of Switched Nonlinear Systems With Unmodeled Dynamics. *IEEE Access*. 2020; 8: 204782-204790. doi: 10.1109/access.2020.3023726
21. Ahrens JH, Khalil HK. High-gain observers in the presence of measurement noise: A switched-gain approach. *Automatica*. 2009; 45(4): 936-943. doi: 10.1016/j.automatica.2008.11.012
22. Hammouri H, Targui B, Armanet F. High gain observer based on a triangular structure. *International Journal of Robust and Nonlinear Control*. 2002; 12(6): 497-518. doi: 10.1002/rnc.638
23. Astolfi D, Marconi L, Praly L, et al. Low-power peaking-free high-gain observers. *Automatica*. 2018; 98: 169-179. doi: 10.1016/j.automatica.2018.09.009
24. Shen Y, Zhang D, Xia X. Continuous output feedback stabilization for nonlinear systems based on sampled and delayed output measurements. *International Journal of Robust and Nonlinear Control*. 2015; 26(14): 3075-3087. doi: 10.1002/rnc.3491
25. Fridman E. Tutorial on Lyapunov-based methods for time-delay systems. *European Journal of Control*. 2014; 20(6): 271-283. doi: 10.1016/j.ejcon.2014.10.001
26. Geravand M, Korondi PZ, Werner C, et al. Human sit-to-stand transfer modeling towards intuitive and biologically-inspired robot assistance. *Autonomous Robots*. 2016; 41(3): 575-592. doi: 10.1007/s10514-016-9553-5

27. Sultan N, Mughal AM, Islam MN ul, et al. High-gain observer-based nonlinear control scheme for biomechanical sit to stand movement in the presence of sensory feedback delays. *PLOS ONE*. 2021; 16(8): e0256049. doi: 10.1371/journal.pone.0256049
28. Chiba R, Takakusaki K, Ota J, et al. Human upright posture control models based on multisensory inputs; in fast and slow dynamics. *Neuroscience Research*. 2016; 104: 96-104. doi: 10.1016/j.neures.2015.12.002
29. Ashyralyev A, Agirseven D. Bounded solutions of nonlinear hyperbolic equations with time delay. *Electronic Journal of Differential Equations*. 2018; 2018(21): 1-15.
30. Mughal AM, Iqbal K. Fuzzy optimal control of sit-to-stand movement in a biomechanical model. *Journal of Intelligent & Fuzzy Systems*. 2013; 25(1): 247-258. doi: 10.3233/ifs-2012-0632